

# Mathematical modelling and process optimization of a continuous 5-stage bioreactor cascade for production of poly[-(*R*)-3-hydroxybutyrate] by *Cupriavidus necator*

Predrag Horvat · Ivna Vrana Špoljarić ·  
Markan Lopar · Aid Atlić · Martin Koller ·  
Gerhart Brauneegg

Received: 12 October 2012 / Accepted: 22 October 2012  
© Springer-Verlag Berlin Heidelberg 2012

**Abstract** A multistage system for poly(hydroxyalkanoate) (PHA) production consisting of five continuous stirred tank reactors in series (5-CSTR) with *Cupriavidus necator* DSM 545 as production strain was modelled using formal kinetic relations. Partially growth-associated production of PHA under nitrogen limited growth was chosen as modelling strategy, thus the Luedeking-Piret's model of partial growth-associated product synthesis was applied as working hypothesis. Specific growth rate relations adjusted for double substrate (C and N source) limited growth according to Megee et al. and Mankad-Bungay relation were tested. The first stage of the reactor cascade was modelled according to the principle of nutrient balanced continuous biomass production system, the second one as two substrate controlled process, while the three subsequent reactors were adjusted to produce PHB under continuous C source fed and nitrogen deficiency. Simulated results of production obtained by the applied mathematical models and computational optimization indicate that PHB productivity of the whole system could be significantly increased (from experimentally achieved  $2.14 \text{ g L}^{-1} \text{ h}^{-1}$  to simulated  $9.95 \text{ g L}^{-1} \text{ h}^{-1}$ ) if certain experimental

conditions would have been applied (overall dilution rate, C and N source feed concentration). Additionally, supplemental feeding strategy for switching from batch to continuous mode of cultivation was proposed to avoid substrate inhibition.

**Keywords** Continuous production · *Cupriavidus necator* · Mathematical modelling · Multistage fermentation · Poly (3-hydroxybutyrate)

## Introduction

Poly(hydroxyalkanoates) (PHAs) constitute a family of biodegradable intracellular polyesters synthesized by a wide range of archaea and eubacterial genera [1–3]; biologically PHAs mainly serve as an intracellular energy reservoir and C source [4]. In addition, a variety of important functions of PHAs in various ecosystems was elucidated during the last years [5]. Among all known PHAs, the homopolymer poly([*R*]-3-hydroxybutyrate) (PHB) constitutes the most widely investigated and best characterized type.

Poly(hydroxyalkanoates) can be biosynthesized from renewable resources (agro-industrial wastes, grains, sugar beet, sugar cane, glycerol from biodiesel production, waste lipids, or whey from dairy industry) by methods of industrial (white) biotechnology [6–8]. By appropriate processing, these polymers can be recovered from the microbial cells and used as sustainable biodegradable substitutes for petrochemical plastics [9–12]. According to Akiyama et al. [13], Harding et al. [14], Pietrini et al. [15], and Titz et al. [16]; the production of PHAs should be more beneficial in terms of a complete cradle-to-gate life cycle analysis (LCA) than in the production of petrochemicals such as

**Electronic supplementary material** The online version of this article (doi:10.1007/s00449-012-0852-8) contains supplementary material, which is available to authorized users.

P. Horvat (✉) · I. Vrana Špoljarić · M. Lopar  
Department of Biochemical Engineering, Faculty of Food  
Technology and Biotechnology, University of Zagreb,  
Pierottijeva 6/IV, HR-10000 Zagreb, Croatia  
e-mail: phorvat@pbf.hr

A. Atlić · M. Koller · G. Brauneegg  
Institute of Biotechnology and Biochemical Engineering,  
Graz University of Technology,  
Petersgasse 12, 8010 Graz, Austria

poly(ethylene) (PE) and poly(propylene) (PP). Unfortunately, PHAs are still inferior to petrochemical plastics considering their costs and, to a certain extent, the material properties [17–19]. Continuous production is a viable strategy for reduction of production costs, and therefore a prerequisite for successful market breakthrough of these biopolymers. Up to date, batch and fed-batch discontinuous fermentations are the most common techniques for microbial PHA production [20–24]. Despite this fact, continuous production mode in biotechnology is a well-known feasible tool for achieving high productivities, lower production costs and constant product (PHAs) quality [25, 26].

The first experiments in this field were published by Wilkinson and Munro [27] as well as by Ramsay et al. [28]. In this paper the authors have described a one-stage chemostat system for production of a poly(3-hydroxybutyrate-co-3-hydroxyvalerate) [P(3HB-co-3HV)] copolymer. Koyama and Doi [29] have produced the same biopolymer with *C. necator* in a one-stage continuous culture from fructose and propionic acid. In these experiments the dilution rate was underlined as a decisive regulation factor for control of the number-average molecular mass ( $M_n$ ) of PHAs (very important for the processing properties). Ackermann and Babel [30] used the two-stage continuous cultivation system for the supply of mixed substrates under controlled conditions during the production phase to prove the mixed substrate concept, and Babel et al. [31] used it for the application of acetic acid as a toxic substrate. In addition, Yu et al. [32] have reported problems with production stability in one-stage chemostat when substrate (propionate) exceeds amount of  $7 \text{ g L}^{-1}$ .

Du et al. [33, 34] have used two CSTRs in series (one predominantly for cell growth, the second one for PHA synthesis) for continuous production of PHA from glucose. By the performed kinetic analysis of the process, the authors calculated reliable data for glucose affinity constant, theoretical yield coefficient of cell mass and maintenance energy coefficient. Also using two-stage cultivation strategies, Jung et al. [35] have reached steady-state conditions for medium-chain-length PHA (*mcl*-PHA) production from alkanes by *Pseudomonas oleovorans* (renamed as *Pseudomonas putida* GPo1). Mothes and Ackermann [36] have obtained the copolymer poly(3-hydroxybutyrate-co-4-hydroxybutyrate) P(3HB-co-4HB) by cultivation of *Delftia acidovorans* P4a on acetic acid and  $\gamma$ -butyrolactone in two CSTRs in series. Recently, high density continuous production of PHB on fructose and urea was described by Khanna and Srivastava [37].

In the past, special attention was devoted to the C/N ratio as regulating factor of PHA synthesis. For continuous P(3HB-co-3HV) production Zinn et al. [25, 38] have applied dual nutrient limitation on non-substitutable

substrates (C and N sources) which was investigated for chemostat cultures by Egli and Quayle [39] and Egli [40]. A high molecular mass at low polydispersities of PHAs was reached under nitrogen limited continuous cultivation of *C. necator* cultivated on mixtures of butyric acid and valeric acid [25]. Furthermore, works of El-Sayed et al. [41], Chakraborty et al. [42], and Wu et al. [43] have confirmed that an optimal C/N ratio must exist to achieve appropriate biopolymer production.

Concerning PHA production kinetic, a strict separation between growth phase and PHA production phase was observed in cultivations of the strain *Pseudomonas* sp. 2F when cultivated on glucose, and also for the facultative methylotrophic bacterium *Methylomonas extorquens* cultivated on by-products of the biodiesel production (non-growth associated PHA formation [44]). Otherwise, it has to be emphasized that some species (i.e. *C. necator*) accumulate PHA to a certain extent already under balanced nutritional conditions (partially growth associated PHA formation); some PHA accumulating strains feature high formation rates for PHA even without any limitation of an essential growth component (full growth associated PHA formation). Such circumstances were reported for the strain *Azohydromonas lata* DSM 1122 (formerly known as *Alcaligenes latus*; [3, 45]), for *Pseudomonas putida* GPo1 ATTC 29347 [3, 46, 47], for synthesis of block-polymers [48] as well as for *Azotobacter vinelandii* UWD [44, 49].

Based on the literature data, Atlić et al. [50] concluded that for aspiring well high productivity as supreme PHA quality, optimal conditions both for cell growth and for PHA accumulation could more easily be achieved in multistage than in single-stage or two-stage continuous bioreactor systems. This is especially valid in the case of non-growth associated PHA producers or partially growth associated PHA producing microorganisms. Implementing previously published engineering approaches [45, 51] which considered a bioreactor cascade of at least five reactors in series as a process-engineering substitute for a continuous plug flow reactor (CPFR), a 5-stage bioreactor cascade system for PHA production was tested by Atlić et al. [50]. The potential of such systems is based on the fact that different controlled nutrient conditions could be applied along the reactor cascade. According to the literature, continuous production mode should result in higher productivities if compared to discontinuous mode, especially due to the fact that, in contrast to discontinuous processes, time needed for preparation and post-processing of the bioreactor and time for the microbial adaptation phase can be eliminated; biomass and product are produced at constant rates and quality during the entire phase of steady state conditions. Further, higher efficiency should be achieved due to the fact that a cascade or plug-flow reactor set-up provides the same productivity at lower residence

time for kinetic ongoings like PHA accumulation [45, 51]. In addition to higher productivities, the multistep cascade features the advantage to trigger the exact process conditions in each step, by the nutrient supply (concentrations of substrates and co-substrates) and parameters like temperature, pH-value and oxygen supply. This is a promising strategy to create novel types of tailor-made biopolymers for special applications, e.g. block-polymers [48] consisting of alternating soft and hard segments. Furthermore, two-stage systems operated at desired dilution rate give more “stretched” residence time and cell age distribution curves than the five-stage system. In N- or P-limited PHB synthesis, the cell age distribution directly correlates with PHB content as well as with molecular mass of polymer, and therefore influences the polydispersity index.

Based on the facts written above, the authors have experimentally tested a continuous five-step stirred tank bioreactor cascade system (5-CSTR) to produce PHB with high molecular mass and low polydispersity index. The five-stage system was designed to provide balanced biomass growth regarding the complete nutrient supply in the first reactor. Subsequently, the second vessel was intended to finalize consumption of nitrogen source so that in this stage growth-associated PHA synthesis should occur. Furthermore, in the last three reactors, the aim was to expose the cells to non-growth associated synthesis of PHA under nitrogen-free conditions in order to increase molecular mass of PHA and to reach a low polydispersity index as well as to collect information about the cellular ability to tolerate permanent long-term N-limitation without serious cell damage or loss of the ability of PHA synthesis.

Under operating conditions (dilution rate for R1 was  $D_1 = 0.139 \text{ h}^{-1}$ ; an overall dilution rate  $D_{\text{TOTAL}} = 0.034 \text{ h}^{-1}$ ), a final concentration of  $81.00 \pm 0.27 \text{ g L}^{-1}$  of cell dry mass (CDM) containing  $77 \pm 7.5 \%$  w/w of PHB and overall PHB productivity  $2.14 \text{ g L}^{-1} \text{ h}^{-1}$  were obtained. In order to provide even better results considering the productivity and production costs, the main issue of this work was to find out whether the applied 5-stage system carries the potential to produce higher concentration of biomass with superior PHB content, along with maintaining the molecular mass at a constant and high level, as well as sustaining the favourably low polydispersity of PHB. The purpose of this work was to optimize the continuous 5-step PHA production system using formal-kinetic mathematical modelling, especially considering dilution rate, productivity, growth rate and nutrient (C and N source) concentrations. This approach should reduce the number of needed experiments on laboratory scale concerning strain treatment, technological set-up and process design which is needed to draw well-grounded conclusions about the ultimate potential of the 5-CSTR for PHA production aiming at higher productivity compared to the basic experiments reported by Atlić et al. [50].

## Materials and methods

The data about the continuous cultivation system, micro-organism, fermentation experiments and related results were reported earlier [50]. The reactor cascade system is presented in Fig. 1. Three different fermentations (FM1, FM2, FM3) which differ in operational characteristics (working volumes, feeding modes, inflows, dilution rates and C/N ratio; Table 1) were modelled according to principles described below and presented in Fig. 2.

### Modelling principles

- Residual biomass (non-PHB part of biomass) is synthesized from glucose and ammonia as C and N sources, respectively. The growth rate is determined by nitrogen and by glucose concentration; the nitrogen depletion causes termination of biomass growth and predominant PHA formation.
- The intracellular product (PHB) is synthesised from glucose; this occurs partly during the phase of balanced biomass growth (growth associated synthesis) and predominantly in the non-growth phase (non-growth associated PHA synthesis). High nitrogen source concentration is applied as an inhibitory regulator of non-growth-associated PHB synthesis. The Luedeking–Piret model [52] of partial growth-associated product synthesis was chosen as the modelling strategy.
- A part of the C source (glucose) is converted to  $\text{CO}_2$  and other minor metabolites, such as excreted organic acids.
- Previously conducted kinetic analysis was performed to determine the basic model parameters.
- Two specific growth rates' relations to substrate concentrations (C; N) have been tested: “double Monod” term according to Megee et al. [53] and Mankad-Bungay relation for double substrate limited growth according to Mankad and Bungay [54].

### Mathematical model

The basic formal kinetic model with growth-associated and non-growth-associated PHB synthesis under nitrogen limitation was adopted from Koller et al. [55]. The model was restructured according to the applied 5-step continuous mode of fermentation (Fig. 1).

The mathematical model consists of 20 differential mass balance equations (Table 1) related to substrate ( $S_n$ ), product ( $P_n$ ), nitrogen ( $N_n$ ) and residual biomass ( $X_n$ ) concentrations ( $n = 1-5$ , position of reactor in the cascade).

**Fig. 1** Five-step bioreactor cascade for continuous PHB production as used in the experiments performed by Atlíć et al. [50]

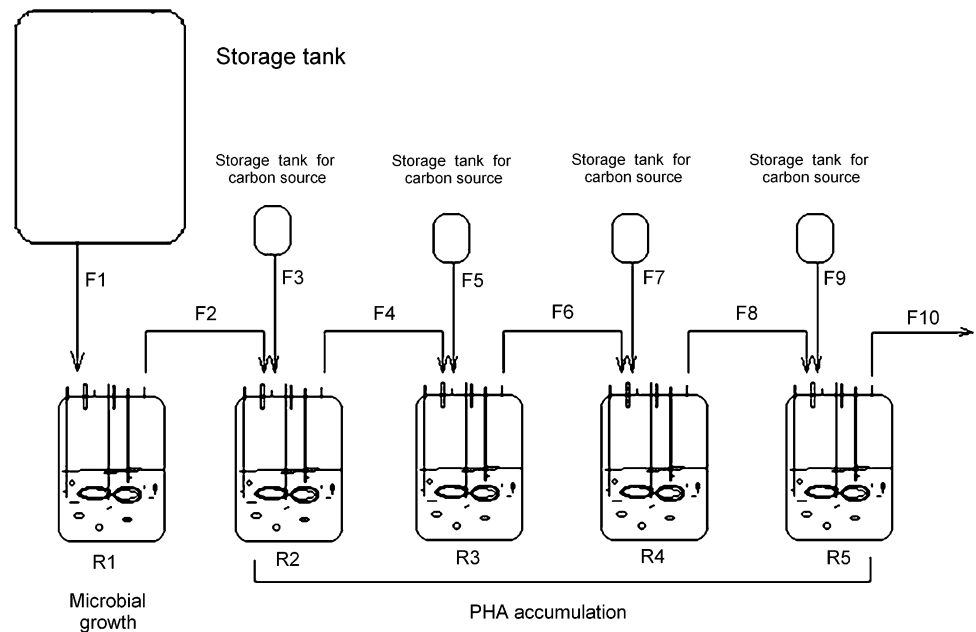


**Table 1** Model equations for PHB production in a 5-stage reactor cascade (5-CSTR)

Equation	Bioreactor (step)
<b>Biomass</b>	
$\frac{dX_{r1}}{dt} = \left(\frac{F_{1,in}}{V_1}\right) X_{r0} - \left(\frac{F_{1,out}}{V_1}\right) X_{r1} + \mu_1 X_{r1}$	$n = 1$
$\frac{dX_{rn}}{dt} = \left(\frac{F_{n-1,in}}{V_n}\right) X_{rn-1} - \left(\frac{F_{n,out}}{V_n}\right) X_{rn} + \mu_n X_{rn}$	$n = 2-5$
<b>Product (PHB)</b>	
$\frac{dP_1}{dt} = \left(\frac{F_{1,in}}{V_1}\right) P_0 - \left(\frac{F_{1,out}}{V_1}\right) P_1 + (\mu_1 m_{P,X} + a_1) X_{r1}$	$n = 1$
$\frac{dP_n}{dt} = \left(\frac{F_{n-1,in}}{V_n}\right) P_{n-1} - \left(\frac{F_{n,out}}{V_n}\right) P_n + (\mu_n m_{P,X} + a_n) X_{rn}$	$n = 2-5$
<b>Substrate</b>	
$\frac{dS_1}{dt} = \left(\frac{F_{1,in}}{V_1}\right) S_0 - \left(\frac{F_{1,out}}{V_1}\right) S_1 - \mu_1 \left(\frac{X_{r1}}{m_{X,S}}\right) - (\mu_1 m_{P,X} + a_1) \left(\frac{X_{r1}}{m_{P,S}}\right) - b_1 X_{r1}$	$n = 1$
$\frac{dS_n}{dt} = \left(\frac{F_{n-1,in}}{V_n}\right) S_{n-1} - \left(\frac{F_{n,out}}{V_n}\right) S_n + \left(\frac{F_{2n-1}}{V_n}\right) S_f - \mu_n \left(\frac{X_{rn}}{m_{X,S}}\right) - (\mu_n m_{P,X} + a_n) \left(\frac{X_{rn}}{m_{P,S}}\right) - b_n X_{rn}$	$n = 2-5$
<b>Nitrogen source</b>	
$\frac{dN_1}{dt} = \left(\frac{F_{1,in}}{V_1}\right) N_0 - \left(\frac{F_{1,out}}{V_1}\right) N_1 - \mu_1 \left(\frac{X_{r1}}{m_{X,N}}\right)$	$n = 1$
$\frac{dN_n}{dt} = \left(\frac{F_{n-1,in}}{V_n}\right) N_{n-1} - \left(\frac{F_{n,out}}{V_n}\right) N_n - \mu_n \left(\frac{X_{rn}}{m_{X,N}}\right)$	$n = 2-5$
<b>Cell dry mass</b>	
$CDM_n = X_{rn} + P_n$	$n = 1-5$
<b>Kinetic equations</b>	
Specific growth rate (double Monod relation according to Megee et al. [53])	$n = 1-5$
$\mu_n = \mu_{Max} \left(\frac{S_n}{S_n + K_S}\right) \left(\frac{N_n}{N_n + K_N}\right)$	
Specific growth rate (according to Mankad and Bungay [54])	$n = 1-5$
$\mu_n = \mu_{Max} \left(\frac{S_n}{S_n + K_S}\right) \left(\frac{N_n}{N_n + K_N}\right) \left(\frac{2K_S K_N}{K_S N_n + K_N S_n} + 1\right)$	
Specific substrate consumption rate (for CO <sub>2</sub> and minor metabolites) $b_n = b_{Max} \left(\frac{S_n}{S_n + K_S}\right)$	$n = 1-5$
Specific growth non-associated PHB production rate $a_n = a_{Max} \left(\frac{S_n}{S_n + K_{aS}}\right) \left(\frac{K_{in}}{N_n + K_{in}}\right)$	$n = 1-5$

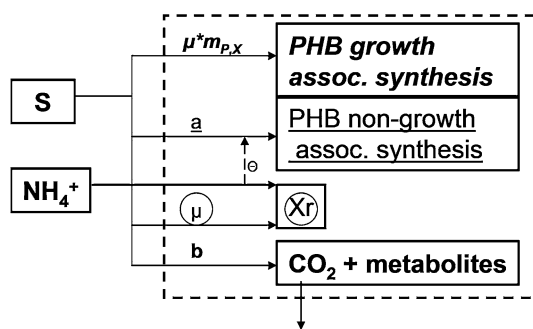


**Fig. 2** Formal kinetic model of PHB synthesis and related kinetic parameters. Full arrows represent metabolic fluxes; dashed arrows represent regulatory influences

Initial values (INIT), hydraulic flows ( $F_1$ – $F_{10}$ ), tank volumes ( $V_1$ – $V_5$ ), substrate concentrations related to the inlet streams ( $S_0$ ,  $S_f$ ,  $N_0$ ), stoichiometric factors ( $m_{P,S}$ ,  $m_{X,S}$ ,  $m_{X,N}$ ,  $m_{P,X}$ ) and kinetic parameters (saturation and inhibition constants, maximal specific growth, production and substrate consumption rates) are listed and explained in Table 2. Kinetic parameters were obtained through kinetic analysis of experimental data originated from cultivation FM1 reported earlier [50]. Mathematical model was validated by simulation of two additional cultivations (FM2 and FM3) [56] operated with different operational characteristics (different substrate feedings, inflows, C/N ratio, dilution rates, working volumes; Table 2).

Before the modelling process, the model sensitivity to parameter changes was computationally tested according to procedures described by Oosterhuis and Kossen [57] and Mayr et al. [58, 59]. Afterwards, the continuous biotechnological system was simulated for the steady states (after 23, 29 and 32 h of batch mode for FM1, FM2 and FM3, respectively) by Berkeley-Madonna quick solver using four-step Runge–Kutta numerical integration method for solving differential equations. This software package was used for all modelling and simulation procedures in this work. Simulated results were adjusted for steady state conditions to the basic experimental data obtained by Atlić et al. [50] for FM1 and by Atlić [56] for FM2 and FM3. Here, the method of least squares was applied, where the sum of squared differences between experimental and simulated values was minimized.

#### Optimization of 5-stage continuous PHB production system

In order to boost PHB production and productivity with minimum experimental efforts, the established mathematical model was used to optimize operational and kinetic conditions. The pre-set goals were arranged as follows:

1. In the first reactor (R1), the maximal productivity of biomass synthesis should be achieved. For this purpose the dilution rate  $D_1 = F_1/V_1$  of R1 should not be higher than the maximal specific growth rate ( $\mu_{\max} = 0.25 \text{ h}^{-1}$ ). According to this condition, the maximal theoretical main inflow ( $F_1$ ) was fixed to  $0.4 \text{ L h}^{-1}$ . Related concentrations of substrates in  $F_1$  ( $S_0$  and  $N_0$ ) were adjusted to the values at which the maximal productivity of reactor was ensured (high  $F_1 \cdot X_{r1}/V_1$  value) without limitation of growth rate caused by oxygen transfer rate. Biomass productivity in R1 was maximized using equation:

$$Pr_{xrl} = D_{1,\text{optimal}} \cdot X_{r1};$$

where

$$D_{1,\text{optimal}} = \mu_{\text{Max}} \left[ 1 - \left( \frac{K_s}{K_s + S_0} \right)^{0.5} \right]$$

Dilution rate  $D_{1,\text{optimal}}$  was used to calculate related inflow  $F_{1,\text{optimal}}$  ( $0.3723 \text{ L h}^{-1}$ ). To stay stable during long-term continuous production, a slightly lower (4.2 %) dilution rate than  $D_{1,\text{optimal}}$  and related  $F_1$  ( $0.3567 \text{ L h}^{-1}$ ) were adopted.

2. In the second reactor (R2) the nitrogen source should be consumed to the level at which inhibition of the PHB synthesis does not take place.
3. In bioreactors R3, R4 and R5, the C source concentration was adjusted by *in silico* feeding enhancement ( $F_3$ ,  $F_7$  and  $F_9$ ) in order to reach maximal value of specific non-growth-associated PHB production rate:  $a_n = f(S_n, N_n) = \text{maximal}$  ( $n = 3, 4, 5$ ).
4. Optimization procedure was performed by tools for multiple parameter optimization in Berkeley Madonna software package, which are able to find absolute minima/maxima of given expression.

## Results and discussion

### Modelling of cultivation FM

Cultivation FM1 [50] was performed in such a way that every reactor in the system (R1–R5) is fed with C source (glucose). The main stream  $F_1$  was added in R1 and the much lower inflows (with high concentration of C source) were added to the R2–R5 (in order to minimize changes of dilution rates in these reactors). In this experiment, nitrogen source was added only in R1 through the main stream ( $F_1$ ). Results of mathematical modelling of this fermentation are presented in Figs. 3, 4 and in Online Resource 1.

**Table 2** Reactor volumes, operating conditions, stoichiometric coefficients and values of adjustable parameters used for mathematical simulation of the 5-stage PHB fermentations

Symbol	Cultivation experiments				Units	Description of symbols
	FM1		FM2	FM3		
	Set 1	Set 2	Set 3	Set 4		
$V_1$	1.6	1.6	1.18	1.16	L	Working volume of reactor R1
$V_2$	1.6	1.6	1.26	1.36	L	Working volume of reactor R2
$V_3$	1.7	1.7	1.27	1.3	L	Working volume of reactor R3
$V_4$	1.7	1.7	1.2	1.36	L	Working volume of reactor R4
$V_5$	2.4	2.4	2.1	1.13	L	Working volume of reactor R5
$F_1$	0.222	0.222	0.1557	0.1587	L h <sup>-1</sup>	Inflow in reactor R1
$F_3$	0.0196	0.0196	0.0178	0.0341	L h <sup>-1</sup>	Feed inflow in reactor R2
$F_5$	0.0223	0.0223	0.0113	0	L h <sup>-1</sup>	Feed inflow in reactor R3
$F_7$	0.0219	0.0219	0.0121	0.0253	L h <sup>-1</sup>	Feed inflow in reactor R4
$F_9$	0.0205	0.0205	0.0177	0	L h <sup>-1</sup>	Feed inflow in reactor R5
$S_0$	67	67	70	63.3	g L <sup>-1</sup>	Concentration of glucose in F1
$S_{f3}$	500	500	517.5	536.8	g L <sup>-1</sup>	Concentration of glucose in F3
$S_{f5}$	500	500	500	0	g L <sup>-1</sup>	Concentration of glucose in F5
$S_{f7}$	500	500	560.8	523.5	g L <sup>-1</sup>	Concentration of glucose in F7
$S_{f9}$	500	500	548.3	0	g L <sup>-1</sup>	Concentration of glucose in F9
$N_0$	4	4	4.7	4.45	g L <sup>-1</sup>	Nitrogen concentration in F1 (added as NH <sub>4</sub> OH)
$P_0$	0	0	0	0	g L <sup>-1</sup>	Concentration of PHB in F1
$X_{r0}$	0	0	0	0	g L <sup>-1</sup>	Concentration of residual biomass in F1
Init. $S_1$	0.2	0.2	13.67	11	g L <sup>-1</sup>	Initial glucose concentration in reactor R1 at start of cont. fermentation
Init. $S_2$	0.2	0.2	13.67	11	g L <sup>-1</sup>	Initial glucose concentration in reactor R2 at start of cont. fermentation
Init. $S_3$	0.2	0.2	13.67	11	g L <sup>-1</sup>	Initial glucose concentration in reactor R3 at start of cont. fermentation
Init. $S_4$	0.2	0.2	13.67	11	g L <sup>-1</sup>	Initial glucose concentration in reactor R4 at start of cont. fermentation
Init. $S_5$	0.2	0.2	13.67	11	g L <sup>-1</sup>	Initial glucose concentration in reactor R5 at start of cont. fermentation
Init. $X_1$	20.7	20.7	18.6	14.5	g L <sup>-1</sup>	Initial residual biomass concentration in reactor R1 at start of cont. fermentation
Init. $X_2$	20.7	20.7	18.6	14.5	g L <sup>-1</sup>	Initial residual biomass concentration in reactor R2 at start of cont. fermentation
Init. $X_3$	20.7	20.7	18.6	14.5	g L <sup>-1</sup>	Initial residual biomass concentration in reactor R3 at start of cont. fermentation
Init. $X_4$	20.7	20.7	18.6	14.5	g L <sup>-1</sup>	Initial residual biomass concentration in reactor R4 at start of cont. fermentation
Init. $X_5$	20.7	20.7	18.6	14.5	g L <sup>-1</sup>	Initial residual biomass concentration in reactor R5 at start of cont. fermentation
Init. $P_1$	6.62	6.62	6.1	5.7	g L <sup>-1</sup>	Initial PHB concentration in reactor R1 at start of cont. fermentation
Init. $P_2$	6.62	6.62	6.1	5.7	g L <sup>-1</sup>	Initial PHB concentration in reactor R2 at start of cont. fermentation
Init. $P_3$	6.62	6.62	6.1	5.7	g L <sup>-1</sup>	Initial PHB concentration in reactor R3 at start of cont. fermentation
Init. $P_4$	6.62	6.62	6.1	5.7	g L <sup>-1</sup>	Initial PHB concentration in reactor R4 at start of cont. fermentation
Init. $P_5$	6.62	6.62	6.1	5.7	g L <sup>-1</sup>	Initial PHB concentration in reactor R5 at start of cont. fermentation
Init. $N_1$	0.01	0.01	0.001	0.84	g L <sup>-1</sup>	Initial nitrogen concentration in reactor R1 at start of cont. fermentation
Init. $N_2$	0.01	0.01	0.001	0.84	g L <sup>-1</sup>	Initial nitrogen concentration in reactor R2 at start of cont. fermentation
Init. $N_3$	0.01	0.01	0.001	0.84	g L <sup>-1</sup>	Initial nitrogen concentration in reactor R3 at start of cont. fermentation
Init. $N_4$	0.01	0.01	0.001	0.84	g L <sup>-1</sup>	Initial nitrogen concentration in reactor R4 at start of cont. fermentation
Init. $N_5$	0.01	0.01	0.001	0.84	g L <sup>-1</sup>	Initial nitrogen concentration in reactor R5 at start of cont. fermentation
$m_{P,S}$	0.998	0.998	0.998	0.998	mol mol <sup>-1</sup>	Stoichiometric coefficient of glucose conversion to PHB
	0.477	0.477	0.477	0.477	g g <sup>-1</sup>	
$m_{X,S}$	1.043	1.043	1.043	1.043	mol mol <sup>-1</sup>	Stoichiometric coefficient of glucose conversion to residual biomass
	0.55	0.55	0.55	0.55	g g <sup>-1</sup>	
$m_{X,N}$	1.015	1.015	1.015	1.015	mol mol <sup>-1</sup>	Stoichiometric coefficient of nitrogen conversion to residual biomass
	6.88	6.88	6.88	6.88	g g <sup>-1</sup>	

**Table 2** continued

Symbol	Cultivation experiments				Units	Description of symbols
	FM1		FM2			
	Set 1	Set 2	Set 3	Set 4		
$m_{p,x}$	0.143	0.143	0.143	0.143	mol mol <sup>-1</sup>	Stoichiometric coefficient of PHB synthesis related to biomass in growth phase
	0.13	0.13	0.13	0.13	g g <sup>-1</sup>	
$\mu_{\max}$	0.82	0.25	0.25	0.25	h <sup>-1</sup>	Maximal specific growth rate
$K_s$	1.585	1.17	1.17	1.17	g L <sup>-1</sup>	Saturation constant for glucose (related to residual biomass growth rate)
$K_n$	0.01509	0.001	0.001	0.001	g L <sup>-1</sup>	Saturation constant for nitrogen
$b_{\max}$	0.18	0.064	0.064	0.064	h <sup>-1</sup>	Maximal specific glucose consumption for maintenance and minor metabolites
$a_{\max}$	0.195	0.23	0.23	0.2	h <sup>-1</sup>	Maximal specific non-growth associated PHB production rate
$K_{in}$	0.009	0.0044	0.0044	0.0044	g L <sup>-1</sup>	Inhibition constant of PHB synthesis (related to nitrogen concentration)
$K_{as}$	0.387	0.605	0.605	5	g L <sup>-1</sup>	Saturation constant for glucose (related to PHB production rate)

Figures 3 and 4 present the results of simulation of the same cultivation in the cases when two different parameter sets were applied (parameter set 1 and 2 from Table 2) and when double Monod term for calculation of specific growth rate was applied (Table 1, equation according to Megee et al. [53]). The use of these two parameter sets has resulted in very similar steady state simulations of the described 5-stage continuous process. They differ regarding the following kinetic parameters: maximal specific growth rate, saturation constants for glucose and nitrogen, maintenance energy, maximal specific non-growth-associated PHB production rate, inhibition constant of PHB synthesis by nitrogen and saturation constant for C source related to PHB production rate. The value of kinetic parameter maximal specific growth rate ( $\mu_{\max}$ ) constitutes the main difference: acceptable simulation results were achieved if  $\mu_{\max} = 0.82 \text{ h}^{-1}$  (parameter set 1, Table 2) was used as well as if  $\mu_{\max} = 0.25 \text{ h}^{-1}$  was applied (parameter set 2; Table 2). The higher value is in disagreement with data presented by Baei et al. [60] where the value of  $\mu_{\max} = 0.17 \text{ h}^{-1}$  was reported for growth of *C. necator* DSM 545 on glucose. Gostomski and Bungay [61] have reported the continuous cultivation of *A. eutrophus* ATCC 17697 on glucose with dilution rates 0.07–0.24 h<sup>-1</sup>. In addition, maximal specific growth rates close to a value of 0.82 h<sup>-1</sup> that were reported are 0.72 h<sup>-1</sup> [62] and 0.81 h<sup>-1</sup> [63, 64] for PHB producers (*R. eutropha*, *A. eutrophus*). The later values were reported for cultivations performed on fructose as C source. On the other hand, reported values of maximal specific growth rate that is very close to the lower value (0.25 h<sup>-1</sup>) used in the work at hands are 0.303 h<sup>-1</sup>, 0.22–0.27 h<sup>-1</sup> and 0.198 h<sup>-1</sup> [10, 37], as well as 0.21 h<sup>-1</sup> [65]. Furthermore, in preliminary experiments and in inoculum cultivations for experiments FM1, FM2 and FM3, values of  $\mu = 0.17$ –0.20 h<sup>-1</sup> were achieved. These values are closer to 0.25 than to 0.82 h<sup>-1</sup>. The

residual biomass concentration was chosen as additional criterion to decide which parameter set (set 1, or set 2) has to be used for further simulations and optimization. Values for simulated residual biomass concentration (calculated as the difference between cell dry matter and PHB concentrations) were in better accordance with experimental data when parameter set 2 (Table 2) was applied for mathematical modelling (result not shown). Therefore, parameter set 2 and the value of maximal specific growth rate of  $\mu_{\max} = 0.25 \text{ h}^{-1}$  were used for further simulations and for process optimization as more reliable and more biologically feasible (if *C. necator* DSM 545 cultivation is performed on glucose). Unfortunately, it was not possible to explain why the model parameter set 1 with value of  $\mu_{\max} = 0.82 \text{ h}^{-1}$  (Table 2) has given satisfying simulation results for CDM and PHB concentration. This situation can happen because of simple “parameter compensation”, a well-known issue in solving of interdependent multi-parametric systems of equations. It has to be considered that the value of  $\mu_{\max} = 0.82 \text{ h}^{-1}$  multiplied with double Monod term, i.e.  $[(S/(K_S + S)) \times (N/(K_N + N))]$  gives values of specific growth rate ( $\mu$ ) which are practically identical with experimentally applied dilution rate ( $D = \mu$ ). The value of  $\mu_{\max} = 0.82 \text{ h}^{-1}$  is perhaps appropriate for simulation of cultivation of *C. necator* on fructose, because an original wild-type strain of *R. eutropha* H16/DSM 529/ is unable to use glucose, but still metabolizes fructose. The strain (DSM 545) used in this work is an UV mutant which has gained the ability to metabolize glucose by mutation. High values of specific growth rate achieved on fructose reported earlier [62, 63] can be considered as a consequence of inherited metabolic ability from the parental strain.

Model parameter set 2 (Table 2) was combined with equation for specific growth rate according to Mankad and Bungay [54]. This relation was applied for the case when the microorganism grows at limited concentration ranges

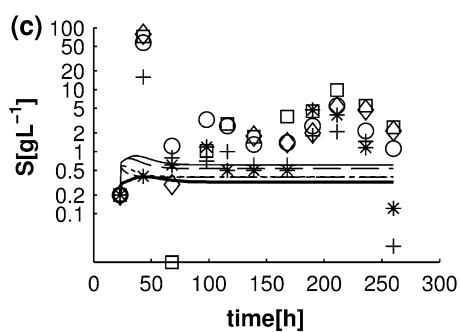
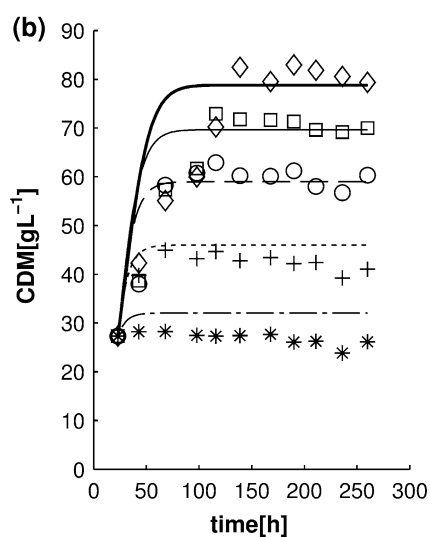
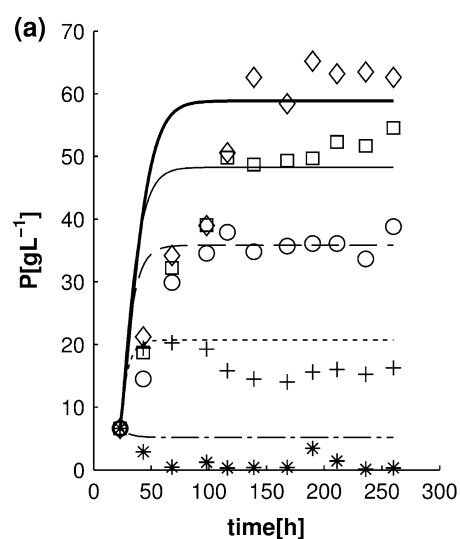


**Fig. 3** Simulated and experimental results for FM1 fermentation: **a** PHB concentration (P); **b** cell dry mass (CDM); **c** glucose concentration (S) (results achieved with parameter set 1; Table 2)

of two substitutable substrates. Later, for double-substrate limited microbial growth, the stoichiometric approach was introduced. This approach, that predicts dual nutrient limitation on non-substitutable substrates for chemostat cultures, has been developed by Egli and Quayle [39], further

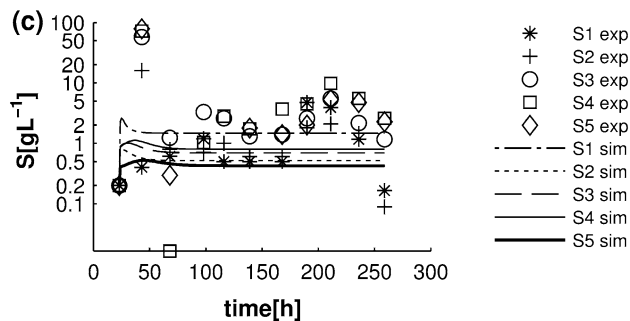
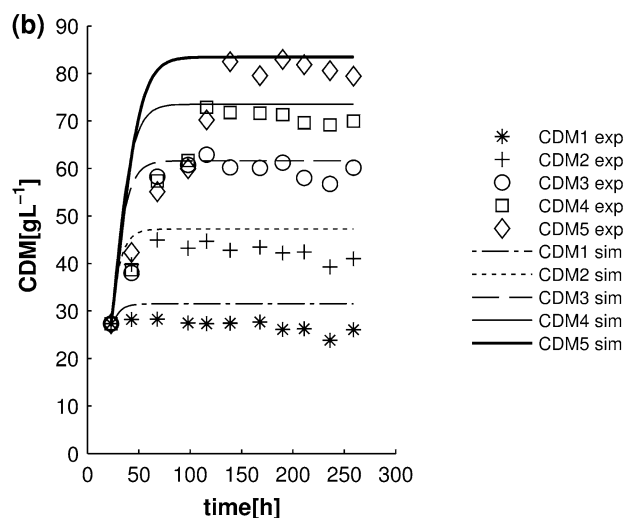
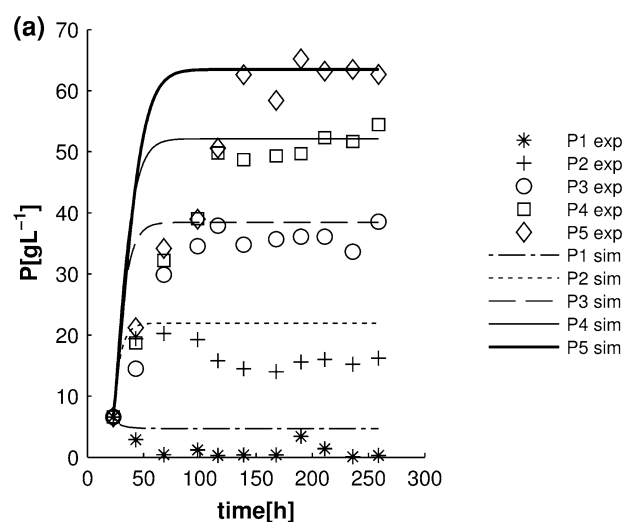


**Fig. 4** Simulated and experimental results for FM1 fermentation with double Monod specific growth relation for **a** PHB concentration (P); **b** cell dry mass (CDM); **c** glucose concentration (S) (results achieved with parameter set 2; Table 2)

advanced by Egli [40] and finally used by Zinn et al. [25, 38]. Egli [40] explains that growth yields do not differ too much between C and N limitation at high growth rates “since the cells do not have the plasticity to adapt to the nutrient limitation like it is the case of low growth rates”.

This is exactly the case in our reactor R1 (biomass growth at high growth rates under presence of both substrates). In R2 the cells were exposed to low concentration of N source and consequently, in reactors R3–R5, to sufficient C source concentration, practically without N source!

If we compare the results of simulations (achieved with two different relations for specific growth rate, dependent on two substrates concentrations), it can be concluded that there is no significant difference in quality of simulations if double Monod (Fig. 4) or Mankad-Bungay (Online Resource 1) specific growth rate relations were used. Therefore, in next steps of this work both mentioned relations for the specific growth rate were used.

Validation of mathematical model (modelling of cultivations FM2 and FM3)

The main criterion for quality of mathematical model is its ability to cover different process conditions and related various metabolic situations (robustness of model). Therefore, the established mathematical model was tested on two additional fermentations (FM2 and FM3) which differ from FM1. Fermentation FM2 was performed in the same way as FM1 but some operational conditions were changed (parameter set 3, Table 2): working volumes, dilution rates, starting concentrations of residual biomass and nitrogen source were lower than in FM1 and glucose concentration at the start of the continuous mode was higher than in FM1. In this fermentation, the glucose feed was similarly arranged as in FM1, but with different inflows resulting in different dilution rates in all reactors. Results of FM2 simulation are shown in Fig. 5.

Kinetic parameters obtained from FM1 and combined with different operational and initial conditions (resulted with set 3; Table 2) have proven to be slightly inappropriate for FM2.

PHB concentrations calculated in the model (Fig. 5a) are not in perfect agreement with experimental data. This is particularly valid for reactors R4 and R5. In contrast, the cell dry matter concentrations are in relatively acceptable agreement with the experiments (Fig. 5b). Surprisingly, the residual biomass concentrations were in good agreement with experimental data (results not shown). Furthermore, shifting of kinetic parameters in the range of  $\pm 10\%$  from applied value in FM1 does not lead to better simulation results. Similar results were achieved in the case when the specific growth rate relation according to Mankad and Bungay [54] has been applied. Based on simulation results achieved for cultivation FM2 it can be concluded that applied kinetic parameters (obtained from FM1) are feasible to provide a relatively fair, but not excellent simulation for cultivations performed under conditions different to FM1. Additionally, it can be mentioned that both

fermentation simulations (FM1 and FM2) give good steady state results, but it seems that the established model is deficient and barely applicable for simulation of transition period of microbial culture when biomass is forced from batch to continuous mode of cultivation (Fig. 4 and Online Resource 1). These simulations are relatively inconsistent at the transition state period (early part of continuous process) which occurs always when a batch process is switched to continuous mode of cultivation. This is a well-known disadvantage of unstructured and formal kinetic models: the response of mathematical model on the changes of crucial variables is usually much faster than the response of real technological/biological system. In order to predict transients correctly, one would need very advanced on-line analytics and a more sophisticated, structured mathematical model.

Fermentation FM3 (set 4; Table 2) was performed in different way than FM1 and FM2: without feed inflows of glucose in R3 and R5 ( $F_5$  and  $F_9 = 0$ ) and with two times higher feed inflows of glucose in R2 and R4 ( $F_3$  and  $F_7$ ) than those used in FM2. Moreover, the ratio of C/N source was lower than in FM1 and FM2. Working volumes were different than in both formerly mentioned fermentations, starting concentration of residual biomass for continuous mode was lower than in FM1 and FM2, while starting concentration of nitrogen source was higher than in FM1 and FM2. Nitrogen source concentration in  $F_1$  inflow stream was higher than in FM1, but lower than in FM2. Simulation results are presented in Fig. 6.

Mathematical simulation of fermentation FM3 using kinetic parameters obtained from the simulation of fermentation FM1 was not able to reach satisfying results comparable with experimental data. Concerning PHB, CDM and substrate concentrations, the mathematical model has provided a satisfying agreement with experimental data only for reactors R1 and R3. Values of simulated variables for reactors R2 and R4 were significantly lower for substrate and slightly higher for PHB and CDM than the experimental values. To achieve satisfactory simulations, it was necessary to change values of maximal specific non-growth-associated PHB production rate ( $a_{\max}$ ) from 0.23 to  $0.2 \text{ h}^{-1}$ , as well as the related saturation constant for glucose (related to PHB synthesis,  $K_{\text{as}}$ ) from 0.605 to  $5.0 \text{ g L}^{-1}$  (set 4; Table 2). When these changes are applied, the simulations of PHB, CDM and substrate concentrations were in good accordance with experimental data for all five reactors. Using values from set 4 (Table 2), the mathematical model has predicted very well the new experimental situation concerning substrate concentrations in all five reactors. This fermentation is characterized by higher steady state glucose concentration in reactors R2 and R4 ( $21$  and  $14.8 \text{ g L}^{-1}$ , respectively) caused by the feeding strategy, as well as with relatively low concentrations of

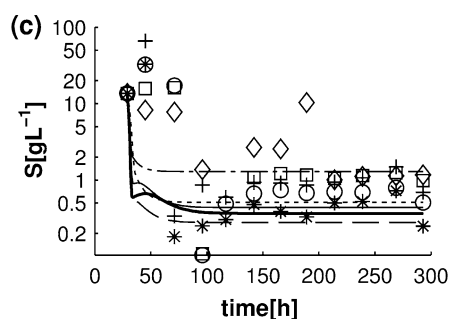
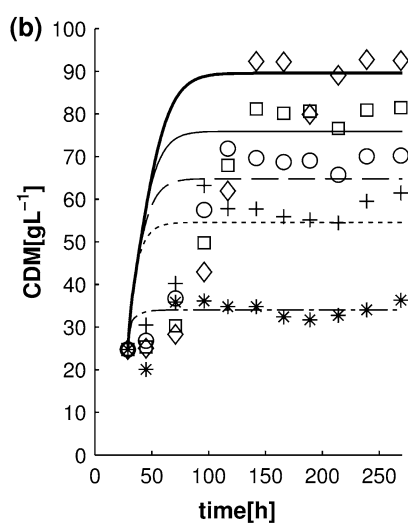
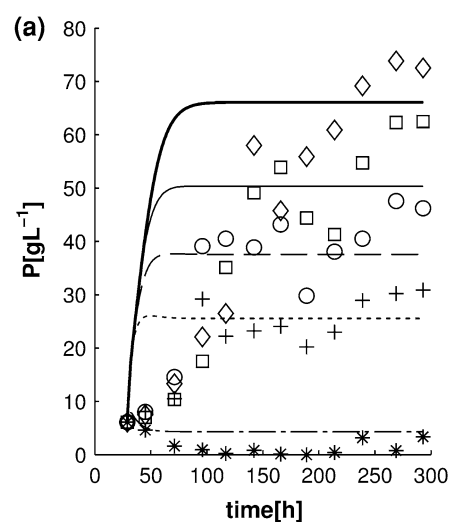


**Fig. 5** Simulated and experimental results for FM2 fermentation: **a** PHB concentration (P) and **b** cell dry mass (CDM); **c** glucose concentration (S). Parameter set 3 (Table 2) with double Monod specific growth relation was applied

C source in reactors R3 and R5 ( $0.28$  and  $1.1 \text{ g L}^{-1}$ ). It seems that the applied feeding strategy negatively influences the microbial substrate consumption ability for PHB synthesis. This situation reflects the change of values of the specific non-growth-associated PHB synthesis rate and the

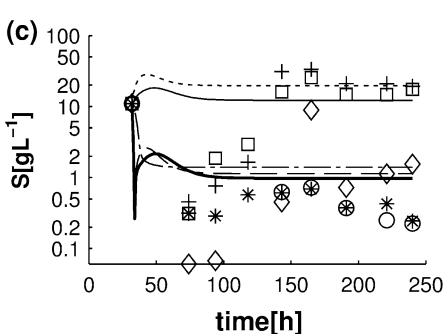
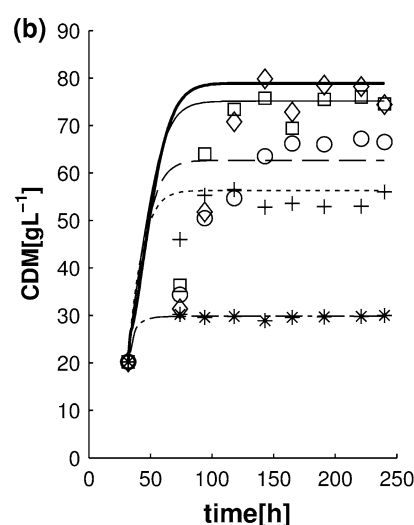
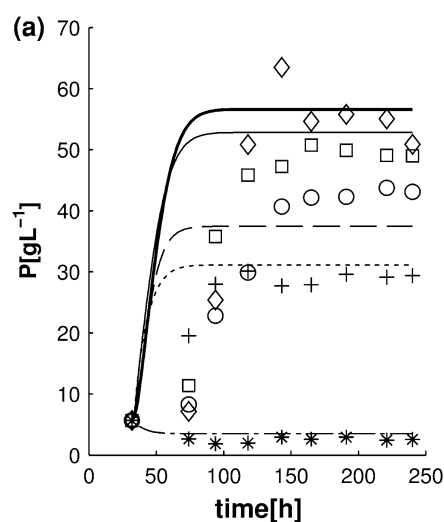


**Fig. 6** Simulated and experimental results for FM3 fermentation (parameter set 4; Table 2): **a** PHB concentration (P); **b** cell dry mass (CDM); **c** glucose concentration (S). Double Monod specific growth rate relation was applied

related saturation constant in model. The case discussed above has not been investigated in details so far. The mentioned feeding strategy was abandoned because of lower final product concentration, PHB content and total productivity (Table 4).

Additionally, both fermentations (FM2 and FM3) were modelled using specific growth rate relation from Mankad and Bungay [54], but this action did not result in significantly better accordance of simulation and experiment (presented in Online Resource 2 and 3).

### Optimization of 5-stage continuous PHB production system

The FM1/FM2 feeding mode (glucose feeding in all reactors) was chosen as a viable PHB production strategy for the 5-stage continuous system. This mode of cultivation has given better PHB and CDM steady state concentrations, better mass fraction of PHB to CDM and higher total productivity (Table 4).

Preliminary investigations of strain *C. necator* DSM 545 have demonstrated that better growth in batch process (using nutrient balanced medium) is observed at a glucose concentration in the range of 20–30 g L<sup>-1</sup>. When concentration of glucose exceeded 30 g L<sup>-1</sup>, a progressive reduction of the growth rate was observed. This is similar to earlier published data for growth of *R. eutropha* on fructose [10]. Mentioned authors have reported concentration values of 60 g L<sup>-1</sup> (fructose), 2 g L<sup>-1</sup> (nitrogen) and 7 g L<sup>-1</sup> (phosphate), as upper limits above which the substrate inhibition of growth occurs. Based on aforementioned facts, the concentration range of 16–30 g L<sup>-1</sup> of glucose was chosen as a desirable steady state range for reactor R1. Within these limits, the value of specific growth rate ( $\mu$ ) lies between 90 and 96.2 % of  $\mu_{max}$  (if sufficient nitrogen is available) and no substrate inhibition occurs. Under conditions of sufficient glucose concentration, the specific non-growth-associated PHB production rate approaches its maximal value ( $a_{max}$ ) if nitrogen concentration does not exceed 0.0025 g L<sup>-1</sup>, so the inhibition of PHB synthesis is practically absent (presented in Online Resource 4). Considering all mentioned facts, the mathematical model was used to predict the 5-stage PHB production in order to achieve better (maximal possible) productivity than in the experiment. To achieve this goal, a parameter set 5 (Table 3) was applied for simulation. Results of simulations are presented in Fig. 7 for “double Monod” as well as in Online Resource 5 for Mankad and Bungay specific growth rate relation.

After optimization, the following can be concluded:

- If optimized values of process variables (parameter set 5, Table 3) are applied, both simulations give practically identical but significantly higher steady state PHB concentration, as well as greater total PHB productivity than in experiments FM1 or FM2 (Table 4; Fig. 7; Online Resource 5);
- Comparing these two simulations there is no significant difference between the end-state values for PHB and substrate concentrations (valid for all reactors);

**Table 3** Optimized process parameters used for mathematical simulation of the 5-stage PHB production reactor system

Adjusted process parameters ↓	Optimized parameter values used in simulation	
	Set 5	Set 6
$F_1$ (L h <sup>-1</sup> )	0.3567	0.3567 if $S_1 < 16$ g L <sup>-1</sup> ; 0 if $S_1 > 20$ g L <sup>-1</sup> ; 0 if $16$ g L <sup>-1</sup> $< S_1 < 20$ g L <sup>-1</sup> and if $dS_1/dt < 0$ 0.3567 if $16$ g L <sup>-1</sup> $< S_1 < 20$ g L <sup>-1</sup> and if $dS_1/dt > 0$
$F_3$ (L h <sup>-1</sup> )	0.1137	0.1137 if $S_1 < 16$ g L <sup>-1</sup> ; 0 if $S_1 > 20$ g L <sup>-1</sup> ; 0 if $16$ g L <sup>-1</sup> $< S_1 < 20$ g L <sup>-1</sup> and if $dS_1/dt < 0$ 0.1137 if $16$ g L <sup>-1</sup> $< S_1 < 20$ g L <sup>-1</sup> and if $dS_1/dt > 0$
$F_5$ (L h <sup>-1</sup> )	0.0986	0.0986 if $S_1 < 16$ g L <sup>-1</sup> ; 0 if $S_1 > 20$ g L <sup>-1</sup> ; 0 if $16$ g L <sup>-1</sup> $< S_1 < 20$ g L <sup>-1</sup> and if $dS_1/dt < 0$ 0.0986 if $16$ g L <sup>-1</sup> $< S_1 < 20$ g L <sup>-1</sup> and if $dS_1/dt > 0$
$F_7$ (L h <sup>-1</sup> )	0.0854	0.0854 if $S_1 < 16$ g L <sup>-1</sup> ; 0 if $S_1 > 20$ g L <sup>-1</sup> ; 0 if $16$ g L <sup>-1</sup> $< S_1 < 20$ g L <sup>-1</sup> and if $dS_1/dt < 0$ 0.0854 if $16$ g L <sup>-1</sup> $< S_1 < 20$ g L <sup>-1</sup> and if $dS_1/dt > 0$
$F_9$ (L h <sup>-1</sup> )	0.0695	0.0695 if $S_1 < 2.5$ g L <sup>-1</sup> ; 0 if $S_1 > 3.5$ g L <sup>-1</sup> ; 0 if $2.5$ g L <sup>-1</sup> $< S_1 < 3.5$ g L <sup>-1</sup> and if $dS_1/dt < 0$ 0.0695 if $2.5$ g L <sup>-1</sup> $< S_1 < 3.5$ g L <sup>-1</sup> and if $dS_1/dt > 0$
$S_0$ (g L <sup>-1</sup> )	243.5	243.5
$N_0$ (g L <sup>-1</sup> )	12.01	12.01
Other parameters	In both sets were used values listed in Table 2; (set 2)	

- Time course of curves in Fig. 7 indicates that steady state values for glucose and PHB concentrations are reached slower when double Monod relation for specific growth rate takes place (if compared with results achieved by Mankad and Bungay relation presented in Online Resource 5);
- In transient period (adaptation of culture after switching from batch mode to continuous process), Mankad and Bungay relation for specific growth rate resulted *in silico* in lower and narrower glucose peaks than double Monod relation. This is very similar to the real experimental situations observed in FM1 and FM2.

Glucose concentration peaks in simulated and *in silico* optimized fermentation (Fig. 7) lie in the range of substrate

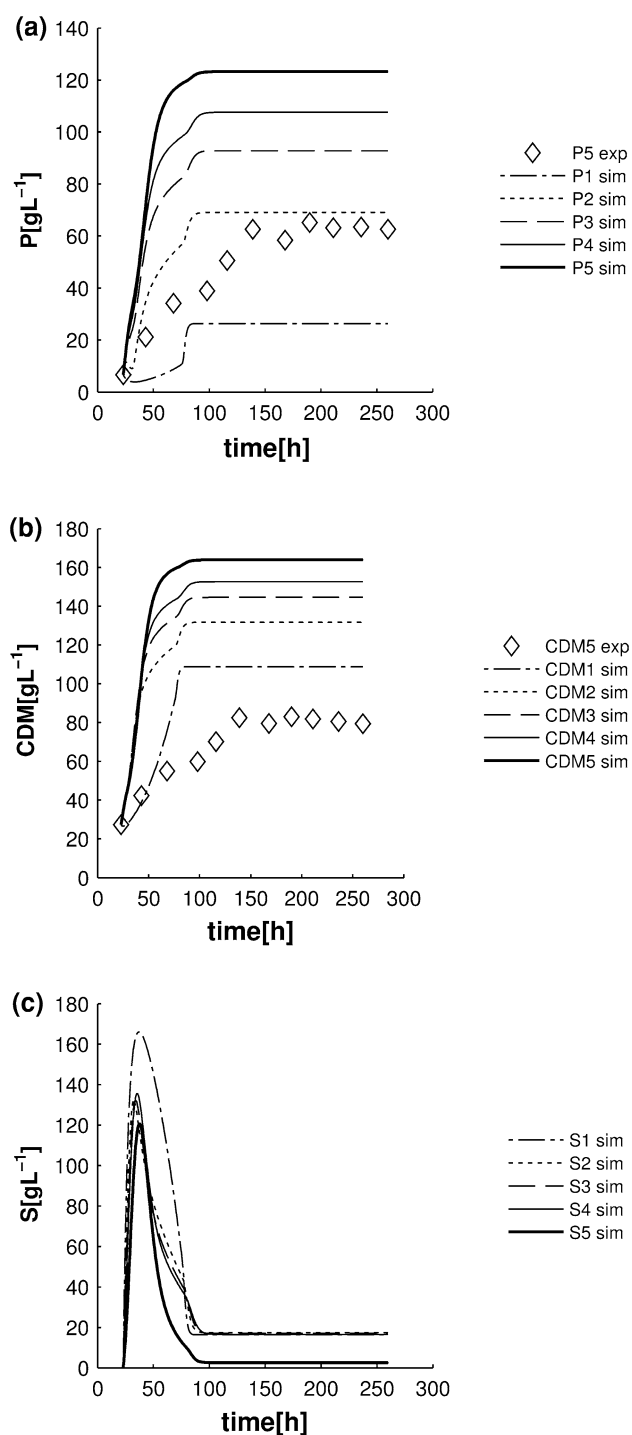


**Fig. 7** Optimized values for **a** PHB concentration (P) and **b** cell dry mass (CDM) with **c** glucose concentration (S) of 5-stage continuous PHB production system when parameter set 5 (Table 3) and double Monod specific growth rate relation were used in simulation. Experimental PHB and CDM data from non-optimized FM1 fermentation are added for comparison

inhibitions. Substrate concentration in the early experimental part of the continuous phase of cultivation could be the reason of why all simulations in this work are “faster in

time” than the performed experiments. Substrate inhibition was not incorporated in the applied model as it was done by Mulchandani et al. [64] and Khanna and Srivastava [10, 37]. In these works, the inhibition term according to Luong [66, 67] was applied.

Since no inhibition is desirable in the real production, we have not developed the mathematical model for that situation. Instead of incorporation of substrate inhibition in the model, another *in silico* strategy of controlled substrate feeding was chosen (i.e. limited feed batch). After switching from batch to continuous mode, the glucose inputs were simulated to be limited by their respective concentrations in reactors. For this purpose glucose feed inflow was set to be active until the concentration of 20 g L<sup>-1</sup> in broth was reached. After that the inflow of glucose has to be stopped until microbial consumption reduces the level of glucose to 16 g L<sup>-1</sup>. This value was set as a “switch on” variable for the next feeding cycle. Applied limits of glucose concentrations (16–20 g L<sup>-1</sup>) keep the specific growth rate in R1 close to  $\mu_{\max}$  and, at the same time, the specific non-growth-associated PHB production rate in R2–R5 is close to its maximal value ( $a_{\max}$ ). Feeding cycles were repeated *in silico* until steady state concentrations of biomass, substrates and product were reached. Afterwards, the simulated system was able to maintain stable continuous mode of cultivation. The described *in silico* scenario corresponds with experimental data for FM1, where the batch grown biomass was adapted during the transient period to conditions of continuous mode of cultivation. The consequence of this adaptation was the increasing of glucose concentration after switching to continuous mode. Similar situations have happened in all fermentations. The simulation of above described optimization of glucose inflow (parameter set 6, Table 3) is presented in Fig. 8 and summarized with other results in Table 4.

The *in silico* achieved result of simulation indicates that substrate inhibition can be avoided if this mode of substrate feeding for transient phase is applied. Finally, *in silico* performed optimizations (with parameter set 5 and 6; Table 3) indicate that PHB productivity, product and CDM concentrations could be significantly boosted in this system (up to 9.95 g L<sup>-1</sup> h<sup>-1</sup>; 123.2 g L<sup>-1</sup>; 163.9 g L<sup>-1</sup>, respectively; Table 4). However, in fermentations FM1 and FM2, the percentage of PHB in CDM was 77.2 and 78.8 %, respectively, but according to *in silico* optimized cultivation, this value would be a little lower (75.2 %). This effect is connected with residence times that are shorter *in silico* than in experiments. Experimental confirmation of aforementioned results (Table 4) will be the subject of future work (dealing with comparison of high-structured metabolic model and just presented formal kinetic model).

**Table 4** Experimental and optimized simulated data for final PHB, CDM and glucose concentrations with achieved productivities for applied 5-stage continuous production system

	Experimental data			Simulated results achieved with optimized parameters		Units
	FM1	FM2	FM3	Set 5 (maximal S concentration wasn't controlled)	Set 6 (maximal S concentration was controlled)	
$D_5$ (dilution rate for R5)	0.13	0.102	0.193	0.307	0.307	$\text{h}^{-1}$
$P_5$ (final output PHB concentration)	62.6	73.2	55.5	123.255	123.237	$\text{g L}^{-1}$
%P (final PHB content related to CDM)	77.2	78.8	70.8	75.2	75.2	% [w/w] $\times$ 100
$F_{10}$ (outflow from R5)	0.306	0.215	0.218	0.724	0.724	$\text{L h}^{-1}$
$F_{10} \times P_5$	19.174	15.709	12.099	89.219	89.205	$\text{g h}^{-1}$
$\text{CDM}_5$	81.1	92.9	78.4	163.94	163.94	$\text{g L}^{-1}$
$S_{5\text{OUT}}$ (average concentration in outflow from R5 for steady state period)	3.55	1.10	3.17	2.54	2.50	$\text{g L}^{-1}$
$Pr_{\text{TOT}}$ (total productivity; related to whole plant volume)	2.139	2.241	1.917	9.957	9.956	$\text{g L}^{-1} \text{h}^{-1}$
$M_w$ (molecular mass)	665	652	595	–	–	kDa
PDI (polydispersity index)	2.6	2.7	2.8	–	–	–
$X_c$ (degree of crystallinity)	68	68	70	–	–	%
$T_m$ (melting temperature)	178	179	180	–	–	$^{\circ}\text{C}$
$T_g$ (glass transition temperature)	2.9	3.1	2.5	–	–	$^{\circ}\text{C}$

In the concentration range of experimentally achieved final values of PHB (FM1, FM2 and FM3), product inhibition was not observable. Therefore, the product inhibition term was not included in the proposed model equations, although that term can be useful if cultivation would be forced in direction of higher PHB content.

In general, through all performed simulations, one additional effect was observed: results for reactors R1 and R2 can be in excellent agreement with experimental data if values of kinetic parameters slightly deviate from sets listed in Table 2. Unfortunately, these changed values of parameters did not give satisfying results for the other three reactors R3–R5. Vice versa, if excellent simulation was achieved for bioreactors R3–R5, applied set of kinetic parameters was not favourable for the simulation of first two reactors in the system. Listed parameter sets (Tables 2, 3) represent some kind of compromise, and they are able to give simulations for all reactors with desired acceptable error.

The problem stated above appears as a consequence of the fact that the metabolic state of cells is not the same in all reactors. This depends on the mean age of the cells, and this is highly dependent on the time that the cells were exposed to nitrogen source starvation. Nitrogen starvation not only affects the redirection of metabolic flux of Ac-CoA towards PHB synthesis but also severely impacts the constitutive and inductive enzyme synthesis; hence, it compromises the enzyme renewal processes and phasins synthesis. According to Park et al. [68], nitrogen limitation causes a decrease in the biosynthesis of biomass precursors

components (among which are amino acid and aspartate—an important precursor for CoA biosynthesis). This causes the decrease in the Ac-CoA concentration and affects cellular growth and PHB production. Furthermore, kinetic parameters (especially specific PHB production rates) are defined in the applied formal kinetic model as constant values that are the same for all reactors, but their values should be related to the metabolic state of cells (which differs with the mean cell age). This situation can be solved by at least two different ways. The first one is an application of high-structured kinetic/metabolic flux models (including incorporation of constitutive and inductive enzyme synthesis, enzyme degradation, kinetics properties of enzymes and cell aging through the reactor cascade). The second one is the introduction of formal kinetic “inhibition” (limitation of PHB synthesis due to cell space “occupation”) or by introducing a time-dependent function of the specific production rate. Because a markedly reduction of the production rate in the previous experiments at a PHB content below the range 75–80 % was not evidenced, this idea needs a further experimental investigation and appropriate computational analysis. The model refinement in this way will be the next step in the work.

Along articles cited earlier, additional data about optimal C/N ratio for PHB synthesis [41–43] could be found in literature, but there is only little information about continuous PHAs production related to data about molecular mass and polydispersity index, its dependencies on dilution rate or about the number of used reactor stages. The average molecular masses of PHB from reactor R5 in FM1,

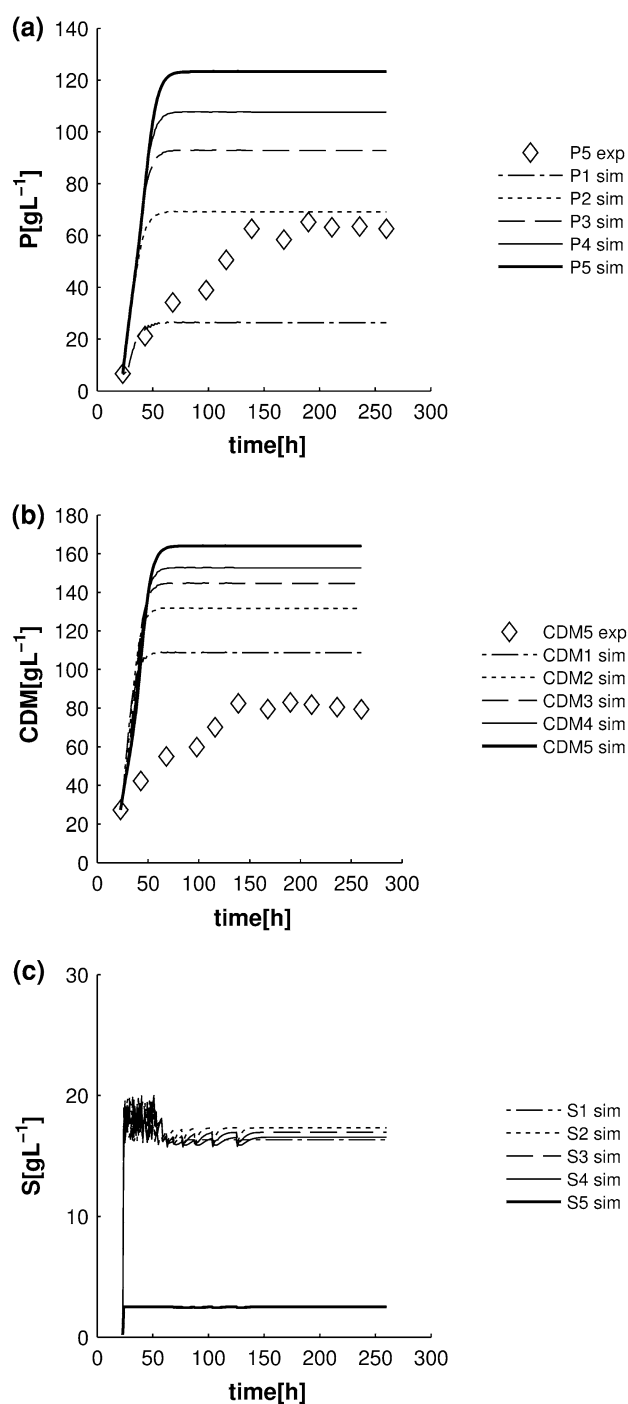


**Fig. 8** Simulated response of the **a** PHB concentration (P), **b** cell dry mass (CDM) and **c** glucose concentration (S) achieved in model using parameter set 6 (Table 3) for 5-stage continuous PHB production system when substrate concentration in reactor was used as leading variable for regulation of feed inflow of glucose (switch on/of boundary values 16 and 20 g L<sup>-1</sup> glucose, respectively)

FM2 and FM3 were 665, 652, 595 kg mol<sup>-1</sup> with polydispersity indices of 2.6, 2.7 and 2.8, respectively (Table 4), [50]. This can be compared with data from Zinn et al. [25] who achieved molecular mass 0.9 and 1.2 MDa,

with polydispersity  $3 \pm 0.3$  so it seems that 5-stage production system has positively influenced the polydispersity index.

## Conclusions

Some important conclusions can be drawn based on all presented results.

- The established mathematical model predicts well the 5-stage continuous PHB production system when glucose is added in all reactors. When glucose is added only in the first, second and in the fourth reactor (residual substrate concentrations are altered), this mathematical model gives a satisfying simulation if two kinetic parameters were changed (maximal specific non-grow-associated PHB production rate and related saturation constant for substrate).
- According to the mathematical simulation, the PHB productivity of the system can be significantly increased (from 2.139 to 9.96 g L<sup>-1</sup> h<sup>-1</sup>) if different experimental conditions are applied (0.08 h<sup>-1</sup>, 12.01 g L<sup>-1</sup> and 150 g L<sup>-1</sup> for overall dilution rate, feed concentrations of nitrogen and glucose, respectively).
- Under experimental conditions of the adaptation period from batch to continuous mode, the C source concentration in the reactors seems to be at a very high level. This could be an inhibitory factor with negative consequence on the microbial growth, known as substrate inhibition. To avoid this kind of problem, substrate concentration in reactor can be triggered by limitation of glucose inflow. In this case, glucose concentration in the reactors can be established as leading regulating variable.
- There is no difference in the simulated end-state values of PHB and CDM concentrations if “double Monod” or Mankad–Bungay relation for specific growth rate is applied in mathematical modelling. But, it seems that Mankad and Bungay relation predicts better the increasing of glucose concentration which appears after switching from batch to continuous mode.
- The oxygen transfer rate of the bioreactor system can be regarded as another limiting variable for the growth rate and subsequently for the PHB productivity. If maximal biomass concentrations as calculated by mathematical modelling can be achieved experimentally, the total consumption rate of dissolved oxygen is expected to be higher than the oxygen transfer rate, hence antagonizing the cell metabolism by oxygen limitation. This obstacle can be easily overcome technically using oxygen-enriched air for gassing the bioreactor.

**Acknowledgments** This work was supported by the Collaborative EU FP7 project ANIMPOL (Biotechnological conversion of carbon containing wastes for eco-efficient production of high added value products; Grant agreement no.: 245084).

## References

- Steinbüchel A, Schlegel HG (1991) Physiology and molecular genetics of poly( $\beta$ -hydroxyalkanoic acid) synthesis in *Alcaligenes eutrophus*. *Mol Microbiol* 5:535–542
- Doi Y, Steinbüchel A (2001) (eds.) Biopolymers, vol. 3b: Polyesters, Wiley-VCH, Weinheim
- Koller M, Salerno A, Miranda de Sousa Dias M, Reiterer A, Braunegg G (2010) Modern biotechnological polymer synthesis—a review. *Food Technol Biotechnol* 48(3):255–269
- Steinbüchel A, Fuchtenbusch B (1998) Bacterial and other biological systems for polyester production. *Trends Biotechnol* 16:419–427
- Koller M, Gasser I, Schmid F, Berg G (2011) Linking ecology with economy: insights into polyhydroxyalkanoate-producing microorganisms. *Eng Life Sci* 11(3):222–237
- Lee SY (1996) Plastic bacteria? Progress and prospects for polyhydroxyalkanoate production in bacteria. *Trends Biotechnol* 14:431–438
- Lee SY (1996) Bacterial polyhydroxyalkanoates. *Biotechnol Bioeng* 49:1–14
- Braunegg G, Koller M, Varila P, Kutschera CH, Bona R, Hermann C, Horvat P, Neto J, Pereira L (2007) Production of plastics from waste derived from agrofood industry. In: Fornasiero Paolo, Graziani Mauro (eds) Renewable resources and renewable energy. University of Trieste, Trieste, pp 119–135
- Reddy CSK, Ghai R, Rashmi KVC (2003) Polyhydroxyalkanoates: an overview. *Bioresour Technol* 87:137–146
- Khanna S, Srivastava A (2005) Recent advances in microbial polyhydroxyalkanoates. *Process Biochem* 40:607–619
- Ren Q, Grubelnik A, Hoerler M, Ruth K, Hartmann R, Felber H, Zinn M (2005) Bacterial poly(hydroxyalkanoates) as a source of chiral hydroxyalkanoic acids. *Biomacromolecules* 6:2290–2298
- Chen CQ (2009) A microbial polyhydroxyalkanoates (PHA) based bio- and materials industry. *Chem Soc Rev* 38:2434–2446
- Akiyama M, Tsuge T, Doi Y (2003) Environmental life cycle comparison of polyhydroxyalkanoates produced from renewable carbon sources by bacterial fermentation. *Pol Degrad Stabil* 80:183–194
- Harding KG, Dennis JS, von Blottnitz H, Harrison STL (2007) Environmental analysis of plastic production processes: comparing petroleum-based polypropylene and polyethylene with biologically-based poly- $\beta$ -hydroxybutyric acid using life cycle analysis. *J Biotechnol* 130:57–66
- Pietrini M, Roes L, Patel MK, Chiellini E (2007) Comparative life cycle studies on PHB based composites as potential replacement for conventional petrochemical plastics. *Biomacromol* 8:2210–2218
- Titz M, Kettl KH, Shahzad K, Koller M, Schnitzer H, Narodoslawsky M (2012) Process optimization for efficient biomediated PHA production from animal-based waste streams. *Clean Technol Environ Policy* 14:495–503
- Choi J, Lee SY (1999) Factors affecting the economics of polyhydroxyalkanoate production by bacterial fermentation. *Appl Microbiol Biotechnol* 51:13–21
- Sudesh K, Iwata T (2008) Sustainability of biobased and biodegradable plastics. *Clean* 36:433–442
- Koller M, Hesse P, Kutschera C, Bona R, Nascimento J, Ortega S, Agnelli J, Braunegg G (2010) Sustainable Embedding of the Bioplastic Poly-(3-hydroxybutyrate) into Sugarcane Industry: Principles of a Future-Oriented Technology in Brazil.-In: *Polymers-Opportunities and Risks*, vol. II, pp 81–96
- Kim BS, Lee SC, Lee SY, Chang HN, Chang JK, Woo SI (1994) Production of poly(3-hydroxybutyric acid) by fed-batch culture of *Alcaligenes eutrophus* with glucose concentration control. *Biotechnol Bioeng* 43(9):892–898
- Ryu HW, Hahn SK, Chang YK, Chang HN (1997) Production of poly(3-hydroxybutyrate) by high cell density fed-batch culture of *Alcaligenes eutrophus* with phosphate limitation. *Biotech Bioeng* 55:28–32
- Ahn WS, Park SJ, Lee SY (2000) Production of poly(3-hydroxybutyrate) by fed-batch culture of recombinant *Escherichia coli* with a highly concentrated whey solution. *Appl Environ Microbiol* 66:3624–3627
- Nonato RV, Mantelatto PE, Rossell CE (2001) Integrated production of biodegradable plastic, sugar and ethanol. *Appl Microbiol Biotechnol* 57:1–5
- Koller M, Bona R, Braunegg G, Hermann C, Horvat P, Kroutil M, Martinz J, Neto J, Varila P, Pereira L (2005) Production of polyhydroxyalkanoates from agricultural waste and surplus materials. *Biomacromolecules* 6:561–565
- Zinn M, Weilenmann H-U, Hany R, Schmid M, Egli T (2003) Tailored synthesis of poly([R]-3-hydroxybutyrate-co-3-hydroxyvalerate) (PHB/HV) in *Ralstonia eutropha* DSM 428. *Acta Biotechnol* 23:309–316
- Sun Z, Ramsay JA, Guay M, Ramsay BA (2007) Fermentation process development for the production of medium-chain-length poly-3-hydroxyalkanoates. *Appl Microbiol Biotechnol* 75:475–485
- Wilkinson JF, Munro ALS (1967) Influence of growth-limiting conditions on the synthesis of possible carbon and energy storage polymers in *Bacillus megaterium*. In: Powell EO, Evans CGT, Strange RE, Tempest DW (eds) *Microbial physiology and continuous culture*. HMSO, London, pp 173–185
- Ramsay BA, Lomaliza K, Chavarie C, Dubé B, Bataille P, Ramsay JA (1990) Production of poly-( $\beta$ -hydroxybutyric-co- $\beta$ -hydroxyvaleric) acids. *Appl Environ Microbiol* 56:2093–2098
- Koyama N, Doi Y (1995) Continuous production of poly(3-hydroxybutyrate-co-3-hydroxyvalerate) by *Alcaligenes eutrophus*. *Biotechnol Lett* 17:281–284
- Ackermann JU, Babel W (1998) Approaches to increase the economy of the PHB production. *Polymer Degrad Stab* 59:183–186
- Babel W, Ackermann JU, Breuer U (2001) Physiology, regulation, and limits of the synthesis of poly(3HB). In: Babel W, Steinbüchel A (eds.) *Advances in Biochemical Engineering/ Biotechnology*, vol. 71 (Biopolyesters) pp. 125–157
- Yu ST, Lin CC, Too JR (2005) PHBV production by *Ralstonia eutropha* in a continuous stirred tank reactor. *Process Biochem* 40:2729–2734
- Du G, Chen J, Yu J, Lun S (2001) Continuous production of poly-3-hydroxybutyrate by *Ralstonia eutropha* in a two-stage culture system. *J Biotechnol* 88:59–65
- Du G, Chen J, Yu J, Lun S (2001) Kinetic studies on poly-3-hydroxybutyrate formation by *Ralstonia eutropha* in a two-stage continuous culture system. *Process Biochem* 37:219–227
- Jung K, Hazenberg W, Prieto M, Witholt B (2001) Two-stage continuous process for the production of medium-chain-length poly(3-hydroxyalkanoates). *Biotechnol Bioeng* 72:19–24
- Mothes G, Ackermann JU (2005) Synthesis of poly(3-hydroxybutyrate-co-4-hydroxybutyrate) with a target mole fraction of 4-hydroxybutyric acid units by two-stage continuous cultivation of *Delftia acidovorans* P4a. *Eng Life Sci* 5:58–62
- Khanna S, Srivastava A (2008) Continuous production of poly- $\beta$ -hydroxybutyrate by high-cell-density cultivation of *Wautersia eutropha*. *J Chem Technol Biotechnol* 83:799–805

38. Zinn M, Witholt B, Egli T (2004) Dual nutrient limited growth: models, experimental observations, and applications. *J Biotechnol* 113:263–279
39. Egli T, Quayle JR (1986) Influence of the carbon: nitrogen ratio of the growth medium on the cellular composition and ability of the methylotrophic yeast *Hansenula polymorpha* to utilize mixed carbon sources. *J Gen Microbiol* 132:1779–1788
40. Egli T (1991) On multiple-nutrient-limited growth of microorganisms, with special reference to dual limitation by carbon and nitrogen substrates. *Antonie Van Leeuwenhoek* 60:225–234
41. El-Sayed AA, Abdel Hafez AM, Abdelhady M, Khodair TA (2009) Production of polyhydroxybutyrate (PHB) Using Batch and Two-stage Batch Culture Strategies. *Aust J Basic Appl Sci* 3(2):617–627
42. Chakraborty P, Gibbons W, Muthukumarappan K (2005) Conversion of volatile fatty acids into polyhydroxyalkanoate by *Ralstonia eutropha*. *Appl Microbiol* 106:1996–2005
43. Wu ST, Lin YC, Too JR (2009) Continuous production of poly(3-hydroxybutyrate-co-3-hydroxyvalerate): effects of C/N ratio and dilution rate on HB/HV ratio. *Korean J Chem Eng* 26(2):411–416
44. Braunegg G, Genser K, Bona R, Haage G, Schelllauf F, Winkler E (1999) Production of PHAs from agricultural waste material. *Macromol Symp* 144:375–383
45. Braunegg G, Lefebvre G, Renner G, Zeiser A, Haage G, Loidl-Lanthaler K (1995) Kinetics as a tool for polyhydroxyalkanoate production optimization. *Can J Microbiol* 41:239–248
46. Hartmann R, Hany R, Pletscher E, Ritter A, Witholt B, Zinn M (2001) Tailor-made olefinic medium-chain-length poly-[(R)-3-hydroxyalkanoates] by *Pseudomonas putida* GPo1: batch versus chemostat production. *Biotechnol Bioeng* 93:737–746
47. Hartmann R, Hany R, Geiger T, Egli T, Witholt B, Zinn M (2004) Tailored biosynthesis of olefinic medium-chain-length poly-[(R)-3-hydroxyalkanoates] in *Pseudomonas putida* GPo1 with improved thermal properties. *Macromolecules* 37:6780–6785
48. Pederson EN, McChalicher CWJ, Srienc F (2006) Bacterial Synthesis of PHA Block Copolymers. *Biomacromol* 7(6):1904–1911
49. Page WJ, Knosp O (1989) Hyperproduction of Poly-hydroxybutyrate during exponential growth of *Azotobacter vinelandii* UWD. *Appl Environ Microbiol* 55:1334–1339
50. Atlić A, Koller M, Scherzer D, Kutschera C, Grillo-Fernandes E, Horvat P, Chiellini E, Braunegg G (2011) Continuous production of poly-[(R)-3-hydroxybutyrate] by *Cupriavidus necator* in a multi-stage bioreactor cascade. *Appl Microbiol Biotechnol* 91:295–304
51. Moser A (1988) *Bioprocess technology: kinetics and reactors*. Springer, New York
52. Luedeking R, Piret EL (1959) A kinetic study of the lactic acid fermentation: batch process at controlled pH. *J Biochem Microbiol Technol Eng* 4:231–241
53. Megee RD, Drake JF, Fredrickson AG, Tsuchiya HM (1972) Studies in intermicrobial symbiosis *Saccharomyces cerevisiae* and *Lactobacillus casei*. *Can J Microbiol* 1818:1733–1742
54. Mankad T, Bungay HR (1988) Model for microbial growth with more than one limiting nutrient. *J Biotechnol* 7:161–166
55. Koller M, Horvat P, Hesse P, Bona R, Kutschera C, Atlić A, Braunegg G (2006) Assessment of formal and low structured kinetic modeling of polyhydroxyalkanoate synthesis from complex substrates. *Biopr Biosyst Eng* 29:367–377
56. Atlić A (2009) Continuous production of polyhydroxyalkanoates in five-stage bioreactor cascade”. Doctoral thesis for the attainment of the degree “Doktor der technischen Wissenschaften” attained at Graz University of Technology, Austria, 2009
57. Oosterhuis NMG, Kossen NWF (1985) Modelling and scaling-up of bioreactors. In: Brauer H (ed) *Fundamentals of biochemical engineering, biotechnology*, vol 2. Deerfield Beach FL VCH, Weinheim, pp 571–605
58. Mayr B, Horvat P, Moser A (1992) Engineering approach to mixing quantification in bioreactors. *Bioprocess Eng* 8:137–143
59. Mayr B, Horvat P, Nagy E, Moser A (1994) Scale-up on Basis of structured Mixing Models: a new Concept. *Biotechnol Bioeng* 43:195–206
60. Baei MS, Najafpour GD, Younesi H, Tabandeh F, Issazadeh H, Khodabandeh M (2011) Growth kinetic parameters and biosynthesis of polyhydroxybutyrate in *Cupriavidus necator* DSMZ 545 on selected substrate. *CI&CEQ* 17(1):1–8
61. Gostomski PA, Bungay HR (1996) Effect of glucose and  $\text{NH}_4^+$  levels on Poly( $\beta$ -hydroxybutyrate) production and growth in a continuous culture of *Alcaligenes eutrophus*. *Biotechnol Prog* 12:234–239
62. Shahhosseini S (2004) Simulation and optimisation of PHB production in fed-batch culture of *Ralstonia eutropha*. *Process Biochem* 39:963–969
63. Raje P, Srivastava AK (1998) Update mathematical model and fed-batch strategies for poly- $\beta$ -hydroxybutyrate (PHB) production by *Alcaligenes eutrophus*. *Bioresour Technol* 64:185–192
64. Mulchandani A, Luong JHT, Groom C (1989) Substrate inhibition kinetics for microbial growth and synthesis of poly- $\beta$ -hydroxybutyric acid by *Alcaligenes eutrophus* ATCC 17697. *Appl Microbiol Biotechnol* 30:11–17
65. Heinzle E, Lafferty RM (1980) A kinetic model of growth and synthesis of poly- $\beta$ -hydroxybutyric acid (PHB) in *Alcaligenes eutrophus* H16. *European J Microbiol Biotechnol* 11:8–16
66. Luong JHT (1985) Kinetics of ethanol inhibition in alcohol fermentation. *Biotechnol Bioeng* 27:280–285
67. Luong JHT (1987) Generalization of Monod kinetics for analysis of growth data with substrate inhibition. *Biotechnol Bioeng* 29:242–248
68. Park JM, Kim TY, Lee SY (2011) Genome-scale reconstruction and *in silico* analysis of the *Ralstonia eutropha* H16 for polyhydroxyalkanoate synthesis, lithoautotrophic growth, and 2-methyl citric acid production. *BMC Syst Biol* 5:101